

Proceedings of the ASME 10<sup>th</sup> Biennial Conference on Engineering Systems Design and Analysis  
ESDA 2010  
July 12 -14, 2010, Istanbul, Turkey

**ESDA2010-25084**

**RELIABILITY CHARACTERIZATION OF A PIEZOELECTRIC ACTUATOR BASED AVC SYSTEM**

**Marco Mazzola\***

University of Brescia  
Department of Mechanical and Industrial Engineering  
Via Branze, 38  
25123, Brescia (Italy)

**Francesco Aggogeri**

University of Brescia  
Department of Mechanical and Industrial Engineering  
Via Branze, 38  
25123, Brescia (Italy)

**Angelo Merlo**

Ce.S.I. Centro Studi Industriali  
Via Tintoretto, 10  
20093, Cologno M.se (Italy)

**Bernhard Brunner**

Fraunhofer-Institut für Silicidforschung ISC  
Neunerplatz, 2  
D-97082, Würzburg (Germany)

**Maria de la O Rodriguez**

Fundacion Fatronik  
Paseo Mikeletegi, 7 - Parque Tecnológico  
E-20009, San Sebastian (Spain)

**ABSTRACT**

Reliability and Maintainability analyses are becoming an increasing competitive advantage in machine tool design. In particular, the goal of machine tools for Ultra High Precision Machining is to guarantee high specified performances and to maintain them over life cycle time. A structured reliability approach applied to such complex and innovative systems must be integrated in the early phase of the design. In this paper, the reliability characterization of an adjustable platform for micromilling operations is presented. The platform is intended to improve the surface finishing of the workpiece, through a broadband Active Vibration Control device based on high performance piezoelectric multilayer actuators. The study intends to assess the capability of the system to maintain along the life cycle the appropriate reduction of the chattering vibrations without any shape error. By dividing the system through a morphological-functional decomposition, the critical elements are detected and their reliability issues are extensively discussed. Their lifetimes are described through opportune distributions and models. The study is completed by the quantitative reliability prediction of the overall system. Finally, a sensitivity analysis is performed and reliability allocation implications are evaluated to determine the effect of every component on the system reliability characteristics and life cycle cost.

*Keywords:* Ultra High Precision Machining, Reliability & Maintainability analysis, system availability, PZT actuator, active vibration control (AVC).

**INTRODUCTION**

The design of innovative machine tools reflects the behavior of the modern competitive markets, where the customer's expectations dramatically increased. Many researches aim to apply innovative solutions to obtain high machining performances and quality of products, reducing the life cycle cost at the same time.

The manufacturers want to purchase machines with high flexibility, high accuracy, high control and high reliability. Predictive analyses can help both the manufacturer and the customer to negotiate price and warranties on a more solid basis. In particular, micromachining excellence implies innovative solutions able to perform dimension-constrained extremely precise works and to maintain these performances over time. Thus, the design of machine tool systems and components has to find solutions to solve the problems and to increase the performance of the micromachining processes. When an innovative system is studied, it is fundamental that since the early phases of the design the reliability and maintainability objectives are clearly identified [1]. In this

\* Corresponding Author, Phone: (+39) 0303715578, Fax: (+39) 0303702448, Email: francesco.aggogeri@ing.unibs.it

environment, analytical efforts are needed, evaluating every potential problem and failure when the product is yet an idea or a drawing. In this way, the design and the realization of a mechanical system become the result of a structured analytical procedure assessing its quality and reliability [2]. The analysis must deploy and specify the functionality and the maintainability over time, in accordance with customer needs. Integrating reliability fundamentals into the very beginning of the product life needs to follow a well-structured analytical approach using qualitative and quantitative tools. Reliability and Maintainability (hereafter R&M) analysis involves a series of activities and procedures widespread in many industries, where risks are dramatically relevant [3-6]. In this context, integrating the R&M principles since the design stage become a competitive advantage; time-consuming and life cycle cost (LCC) increasing activities at concept and design phases will deal to long-period great savings along the product lifecycle (Fig. 1).

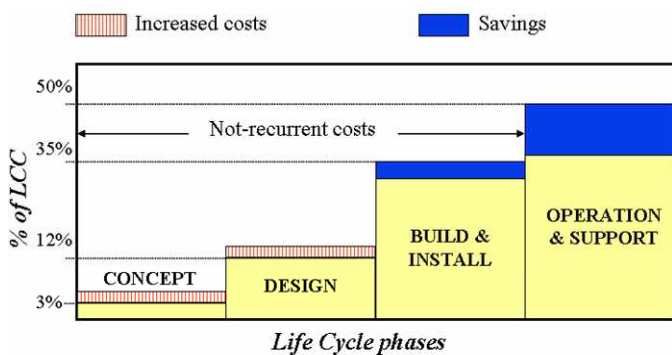


FIGURE 1. R&M approach as a competitive advantage.

In this paper, R&M concepts are applied to the development of a mechanical group. This subsystem is integrated into a micromilling machine. In particular, the authors show the importance of developing a reliability analysis since the early phases of the design, intended to guarantee specified performances and to maintain them over time. The paper resumes the R&M approach, explaining the steps the authors followed to perform a predictive R&M analysis before the prototyping of the product. Different tools widely used for these objective have been shown throughout the paper.

The study focuses on an innovative design of an adjustable Smart platform for micromilling machines. The platform is conceived to improve the surface finishing of the workpiece, through a broad-band Active Vibration Control (hereafter AVC) device based on high performance piezoelectric actuators. The goal is to develop a structured procedure to assess the reliability characteristics of the platform. In this study, the R&M analysis follows two main consequential phases. The first assessment deals with the intrinsic reliability of the design, the feasibility and the capability to obtain specified performances. In fact, for a correct reliability approach, many qualitative analyses must anticipate the reliability characteristics estimation. Preliminary studies are performed to delve into the product functionalities and expected behavior. First of all, the system is broken following a morphological-functional decomposition. In this way, the functions of every component are specified and related with those of the system. Quality Function Deployment and Design

Failure Mode and Effects Analysis (DFMEA) techniques are introduced to evaluate the capability of the platform to accomplish the task it has been designed for, to assess improvement actions to increase machine reliability. Furthermore, these preliminary evidences have to highlight the critical elements that need further analytical efforts in order to predict their reliability behavior. The paper mainly focuses on the second phase, concentrating on the reliability modeling of critical elements and assessing the system capability to maintain the performances over time.

### AVC SYSTEM DESIGN

The subsystem is an innovative platform for Ultra High Precision micromilling Machines. Micromilling operations have to generate outputs characterized by very close tolerances, high precision and surface finishing. During the process, the contact between the cutting tool and the workpiece surface at the tool tip point generates chattering vibrations. Any vibration is recorded on the workpiece surface, directly affecting the roughness. Consequently, uncontrolled vibrations lead to poor surface finishing that is unacceptable in high precision micromachining.

The Smart Platform (hereafter SP) has been conceived to improve the surface finishing of the workpiece, through a broadband AVC device based on high performance piezoelectric actuators [9-10]. The idea of the SP directly derives from the Stewart platform, but it has only three degrees of freedom instead of six. The solution would guarantee a feasible integration with piezoelectric devices. The SP has to connect the machine tool spindle with the ram. It includes two platforms: the fixed platform is directly constrained to the machine tool ram, instead the mobile to the housing of the spindle. Three piezoelectric actuators permit the relative movement of these two platforms, as shown in Fig. 2. When a displacement is measured at the tool tip point, the actuators are dynamically activated in order to compensate the vibrations and to reduce their effects on the workpiece surface.

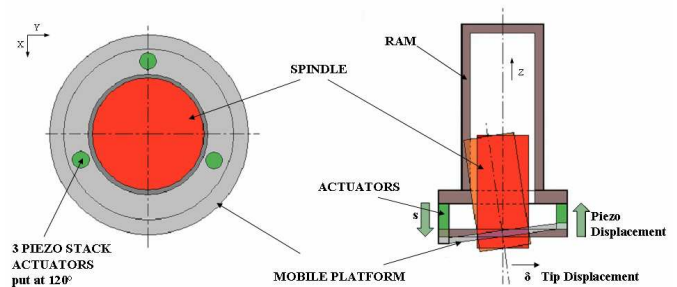


FIGURE 2. Smart platform concept.

Since a piezoelectric cylindrical actuator is able to move in its axial direction, but it becomes extremely frail when moments and/or shear forces are applied, the SP is designed with three degrees of freedom (two rotational in X-Y plane and one translational along Z direction). Once a brief description of the idea has been explained, it is possible to delve into the reliability procedure developed during the early phases of this design.

### Reliability of the SP: preliminary analysis

Any product is considered reliable when it satisfies the functionality along a specified life cycle time. The SP has to accomplish main functions for a life cycle time equal to 10 years (32,000 working hours):

- to compensate the chattering vibrations generated at the tool tip point (correction of the tool position up to  $\pm 20 \mu\text{m}$ )
- to limit the roughness on the workpiece
- to support the task of the machine without any shape errors

The SP works in a traditional micromilling environment: temperature close to  $40^\circ\text{C}$  (anyway less than  $80^\circ\text{C}$ ), plentiful lubrication and frequency between 100 and 300 Hz.

A well-structured reliability approach begins with the breakdown of the entire system into basic elements. This hierarchical development is useful when many elements concur to define the system and their probabilities of failure are different. The SP is divided into the elements outlined in Fig. 3.

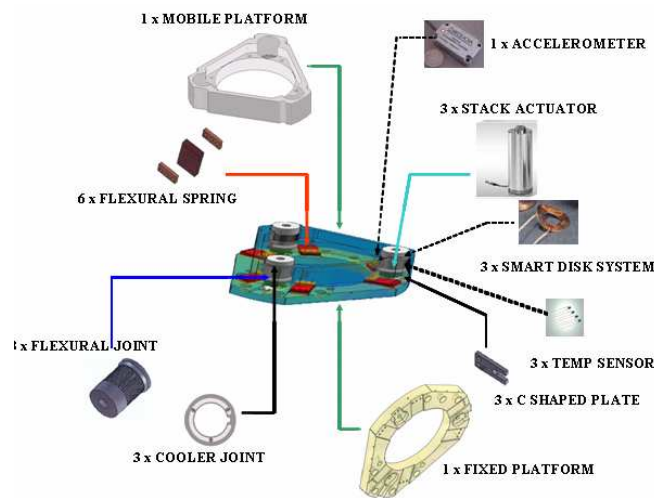


FIGURE 3. SP morphological-functional decomposition.

Every component is designed to accomplish elementary functions. The integration of these functions determines the capability of the system to achieve the technical purposes [2].

The SP can be visualized as an actuation block between two platforms interfacing with the machine tool. The fixed platform in Al alloy connects directly the SP with the machine tool ram. It houses the actuator extremities as well as one side of the flexural springs. The mobile platform, still in aluminum alloy, links the SP with the housing of the spindle. It houses the flexural joints as well as the other side of the flexural springs. The relative movement between the two platforms is permitted by three piezoelectric multilayer stack actuators, strategically positioned on the fixed platform (see Fig. 2). A stroke sensor is integrated in the supplied actuators. A mechanical support system completes the SP, conferring the correct stiffness to the actuator, avoiding undesired stresses and consequent breaks. Every actuator is connected to an innovative flexural joint, designed to avoid torsional and shear stresses to the piezo elements. Furthermore, two flexural springs are positioned close to every actuator. They have been designed to connect the two platforms. Every spring is characterized by high torsional and radial stiffness, but free to smooth in axial direction.

Other support elements complete the mechanics of the system. The SP includes three steel C-shaped plates to locally increase the stiffness, where the fixed platform and the actuators interface. Furthermore, every flexural joint is connected to an aluminum cooler joint, designed to lead compressed air against the actuator surface when the temperature exceeds  $40^\circ\text{C}$ .

Some electronic devices have been integrated in the SP system. A temperature sensor is applied on every actuator surface. Close to every piezo head, two strain gauges are assembled on a steel disk. Finally, an accelerometer measures the displacements of the tool tip to be converted in the correct voltage for piezo motion.

A correlation matrix has been used to identify the most critical elements, looking at their direct influence on the system functionality [11]. Furthermore DFMEA has been applied to the system, both evaluating potential failures due to design lacks (potential infant failure modes) and to deviations from the life cycle (closely related to the Mean Time Between Failure MTBF). A heterogeneous team identified every potential failure mode of the component outlined by the system tree decomposition, so as its effect on the SP functions. Following Ford Machinery DFMEA approach, the Risk Priority Numbers (RPNs) have been calculated for every combination of failure cause-mode-effect. Greater is the RPN value, more seriously the potential failure has to be managed [2, 4, 11, 12].

Table 1 and Tab. 2 resume the results of DFMEA analysis, listing the most severe RPNs, the relative elements and failure mode. Furthermore, it is interesting to specify if the failure should happen during the early beginning of the life cycle (Infant phase) or during the expected operative life (Overall phase). This implies to manage the information differently. If an infant potential failure mode has been noticed, it's urgent to review the design or the design controls. Otherwise the failures influence the reliability of the system and improvement actions must focus on component durability and reliability allocation or on further machinery controls.

TABLE 1. Infant phase DFMEA top RPNs and failure modes.

Element	Failure Mode	RPN	Reduced
PZT	Infant break do to fatigue stress	160	80
FJ	Inappropriate torsional stiffness	144	54
FJ	Doesn't maintain the connection with the mobile platform	144	128
ACC	Doesn't measure the displacement at the tool tip point	140	63
FJ	Doesn't disperse heat	128	64
FJ	Doesn't maintain the connection with the actuator	126	112

The highest RPNs detected for the Infant Phase DFMEA (Tab. 1) have been reduced introducing improvement actions on the design, by reviewing supplier's specifications and material characteristics, and performing FEM analyses. Thus the analytical efforts concentrate on the results of the second DFMEA, directly related to the product behavior along the life cycle (Tab. 2).

Looking at the correlation matrix results [11] and the Overall phase DFMEA top RPNs, the preliminary analysis shows the piezoelectric actuators (PZT), the flexural joints (FJ) and the accelerometer (ACC) are the most critical elements,

whose reliability characterization must be deeply investigated. Their functions are extremely related to those of the SP, thus their reliability modeling directly influence the prediction of the entire system behavior and the life cycle time and cost as a consequence. For this reason, the reliability analysis continues focusing on these components separately. In fact, a correct reliability approach retraced up and down the system tree. The morphological-functional decomposition leads to bottom-level analyses. Once models and evidence are traced for single critical elements, the overall system reliability can be assessed through Reliability Block Diagram technique.

**TABLE 2.** Overall Life cycle DFMEA top RPNs and failure modes.

Element	Failure Mode	RPN
PZT	Break do to fatigue stress	567
FJ	Break do to fatigue stress	441
ACC	Doesn't measure the displacement at the tool tip point	294
FJ	Doesn't maintain the connection with the mobile platform	280
ACC	Wrongly measures the displacement at the tool tip point	252
FJ	Doesn't maintain the connection with the actuator	245
PZT	Displaces inappropriately	120

**Reliability characterization of the flexural joints**

The innovative flexural joint (patented by Ce.S.I.) is a key factor for the functionality of the SP. It is connected to the mobile platform and it is threaded to an actuator on the other side. It is a steel cylindrical device, with the lateral surface partially foliated by long lateral beams that guarantee small stiffness in the transversal direction (Fig. 4). On the other hand, the flexural joint is characterized by very high axial stiffness. In fact, the flexural joint is designed to avoid torsional and shear stresses to the piezo elements, giving more stiffness to the actuator in its longitudinal direction [13].

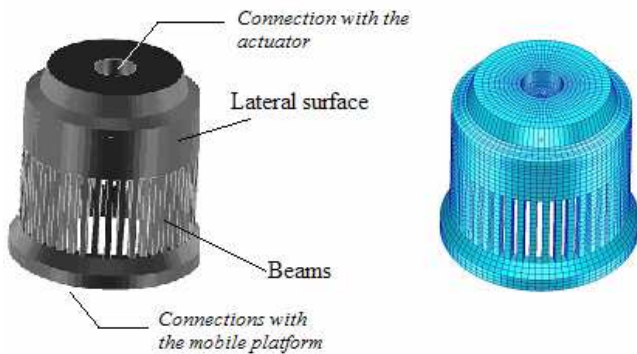


**FIGURE 4.** Scheme of the flexural joint and FE model.

To predict the reliability behavior of a component under specified variable working conditions, a deterministic design could fail to provide the necessary understanding. Since the material characteristics are well known and the structural response to mechanical loads is statistically predictable, a probabilistic approach becomes more suitable for this analysis [6, 14, 15]. A strength-stress analysis is performed to estimate the reliability and the failure rate of the flexural joint [14].

Normal distributions of strength  $S(s)$  (Eq. 1) and stress  $L(s)$  (Eq. 2) are assumed, as shown in Fig. 5.

$$S(s) = \frac{\exp\left[\frac{-(s - \mu_S)^2}{2\sigma_S^2}\right]}{\sigma_S (2\pi)^{0.5}} \tag{1}$$

$$L(s) = \frac{\exp\left[\frac{-(s - \mu_L)^2}{2\sigma_L^2}\right]}{\sigma_L (2\pi)^{0.5}} \tag{2}$$

The mean value  $\mu_S$  of strength for the material can be defined by admissible stress multiplied for a coefficient that involves the fatigue. The standard deviation  $\sigma_S$  is proportional to the mean value [14]. The mean value of stress  $\mu_L$  for the joint can be read directly from results of the FE analysis after an optimization of the geometry. The standard deviation  $\sigma_L$  has been empirically estimated with reference to the load conditions.

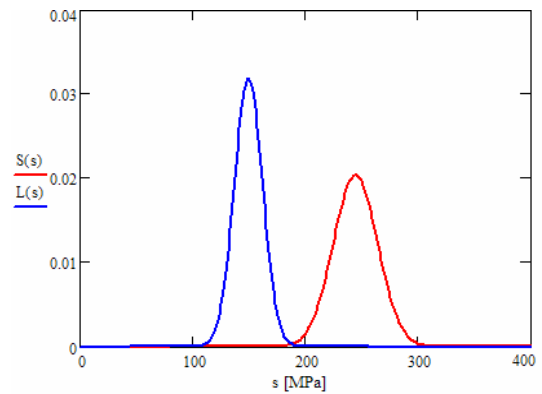


**FIGURE 5.** Strength and stress distributions of the flexural joint.

The mean values, standard deviations and coefficients used in calculating the distributions are listed in Tab. 3. A Safety Margin (Eq. 3) equal to 4.09 is determined [14]. Under the hypothesis that the strength doesn't deteriorate with time and the load is applied 120 times per hours ( $n(t)=120t$ ), Eq. 4 shows the general expression for reliability as a function of time, with distributed load and strength.

**TABLE 3.** Parameters and coefficients for the SS analysis.

Parameter	Assumed value [MPa]
$\mu_S$	0.35*700
$\sigma_S$	0.08*\mu_S
$\mu_L$	150
$\sigma_L$	12.5

When reliability concepts are introduced at design phase, prior to testing campaigns, it is generally accepted that the failures of the system (and of the components too) approximately occur following an exponential distribution along the life cycle time.

This means a constant failure rate, expressed in failures every million hours [3-6].

$$SM = \frac{\mu_s - \mu_L}{\sqrt{\sigma_S^2 + \sigma_L^2}} \quad (3)$$

Failure rate is determined by Eq. 5. After an infant phase (approximately 600 h), the trend of failure rate function becomes asymptotic at 6,800 hours. A constant failure rate of 3.5 failures every million hours is assumed, as an average of the integral of  $\lambda(t)$  function between 600 and 6,800 h (Fig. 6).

$$R(t) = \int_0^\infty \left[ (S(s) \cdot \left( \int_0^s L(s) ds \right)^{n(t)}) \right] ds \quad (4)$$

$$\lambda(t) = -\frac{dR(t)}{dt} * \frac{1}{R(t)} \quad (5)$$

Thus an exponential distribution is used to describe the reliability behavior of the flexural joint, because the infant failures have been discussed and treated separately. The estimated Mean Time To Failure (MTTF) is close to 3E05 h.

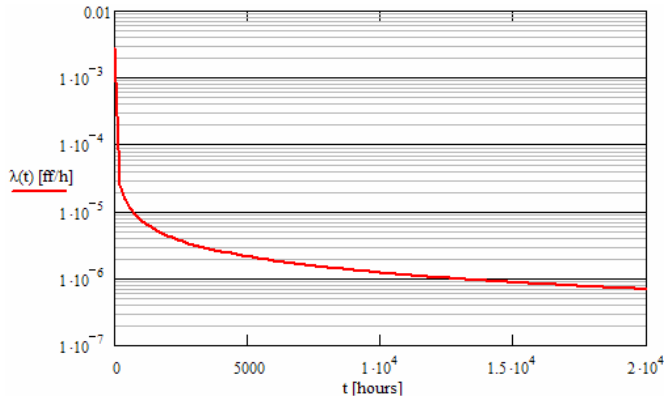


FIGURE 6. Failure rate function for the flexural joint.

### Reliability characterization of the PZT actuators

Piezoelectric devices have become key elements in many applications, such as precision positioning, motions and adaptive mechanical damping. Different types of piezoelectric material and design solutions are available [16-18].

As explained before, the actuators are integrated into the SP to compensate the chattering vibrations, displacing in their axial direction to correct the tool tip position up to  $\pm 20 \mu\text{m}$ . These features address the designers to introduce a high voltage PZT (Lead Zirconate Titanate  $\text{Pb}(\text{Zr},\text{Ti})\text{O}_3$  ceramics) multilayer actuator (Fig. 7). Multilayer piezo actuators offer many advantages compared to other active materials, thus they are increasingly used in various smart applications, contributing to the development of a new field of intelligent structures. A multilayer piezoelectric actuator consists of several single thin

layers stacked on top of one another. This configuration has the great advantage of achieving high displacement proportional to the applied voltage [16-18].

Applying a voltage up to 1,000V, a cylindrical actuator with height and diameter close to 50 mm can generate in its axial direction a maximum force of 50 kN. A maximum stroke of 55  $\mu\text{m}$  is guaranteed, with an ultrahigh acceleration and response time less than 20 ms. Hereafter piezo term always refers to a stack high voltage PZT actuator. The piezoelectric cylindrical actuators are able to move in their axial direction, but they are extremely frail when moments and/or shear forces are applied [16-18]. Furthermore, when high voltages are applied to PZT multilayer materials, tensile stresses reduce the durability and stability due to the delamination of layers and electrodes [16]. For this reason, the actuators designed for high performances and long durations are preloaded. The preload is another important design issue in order to increase the resistance to degradation with a negligible loss of the strain output [20, 21]. In the specific case, the piezo stacks are incorporated into a stainless steel casing, compensating tensile stresses up to 6,000 N (close to 4 MPa), where the piezo becomes extremely vulnerable. In this manner, the elements should always work in a compressive state.

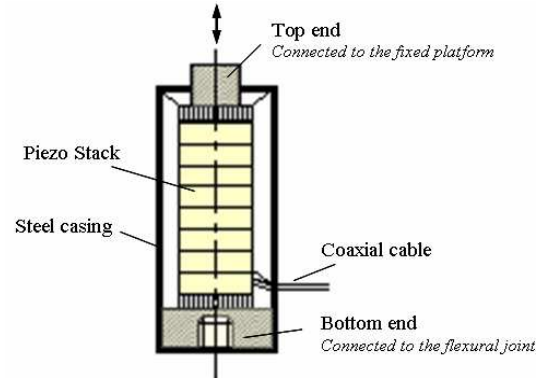


FIGURE 7. Scheme of a piezoelectric multilayer actuator.

There isn't a deterministic formulation to assess the lifetime of piezo actuators because many parameters, such as temperature, humidity, voltage, load and preload, operating frequency and material characteristics, concur to determine piezo durability [16, 21-25]. At design phase, the assessment of piezoelectric device reliability is only supported by the supplier life cycle predictions and quite poor literature [21]. Many works studied the lifetime of piezoelectric actuators, therefore they lack in generalization due to the complexity of the element. These aspects must be evaluated individually for every specific application.

Excluding any processing defects [16, 18], the reliability characterization of the three piezo actuators consider their life cycle under the peculiar operating electro-thermal-mechanical conditions of the SP system. It means that both the properties of the ceramic and coupled issues with the device design influence the lifetime of the piezo stack. Thus a complete understanding of the durability must consider the intrinsic failure of the piezo device (function of frequency, voltage and temperature) and the failures derived from undesired torsional, radial or tensile overstresses [18, 26].

Both the supplier and the literature confirm that a high voltage piezo stack actuator (with specified maximum stroke, load and length) should meanly fail after 5E09 cycles. Consequently, under defined conditions, the lifetime of such an actuator working at a frequency of 150 Hz can be estimated by a MTTF equal to 9,200 h (the ratio between the lifecycles and the frequency expressed in cycles per hour) [11, 27-30].

A quantitative approach can confirm this estimation. Generally, it can be assumed the lifetime  $t$  (expressed in cycles) of ferroelectric devices, working at absolute temperature  $T$  and under an applied electric field  $E$  (kV/mm), can be described by an empirical rule. Equation 6 shows the Black's equation (derived from Arrhenius's one), where  $A$  (cycles mm/kV) and  $n$  are two constants,  $k$  is the Boltzmann's constant and  $W$  is a sort of activation energy [16, 25, 28, 29].

$$t = A E^{-n} \exp(W / kT) \quad (6)$$

In the SP the actuator should work at controlled temperature (meanly 311.15 K, close to the upper limit) and under an average applied electric field of 2kV/mm. Assuming an activation energy of 0.99 eV and the constant values presented by Koh *et al.* [28], a MTTF equal to 5.14E09 cycles (approximately 10,000 working hours) can be estimated.

The reliability characterization of the piezo actuators must comprehend the failures due to overstresses too. The SP has been designed to avoid any kind of torsional, shear and tensile stresses on the actuators. Thus, these failure modes are related to the system design and operation, depending on damages that could happen to the elements demanded to prevent them. A failure occurred to the flexural joint or to the couple of flexural springs directly causes the crack of the actuator. Otherwise, tensile overstresses occur when an excessive displacement is needed and the preload is exceeded as a consequence.

It has been calculated the lifetime of the flexural joint is described by an exponential distribution and a MTTF of 3.5 failures every million hours. Furthermore, it is assumed a constant failure rate equal to 5 failures every million hours for every flexural spring. The probability of failure due to tensile overstress and the relative failure rate is estimated through a stress-strength analysis, following the same approach used for the flexural joint [14]. It is considered the preload ( $\mu_P$  equal to 3.772 MPa and  $\sigma_P$  to  $0.08 * \mu_P$  MPa) and the applied tensile load ( $\mu_T$  equal to 1.257 MPa and  $\sigma_T$  to 0.08 MPa) follow normal distributions (modifying Eq. 1 and Eq. 2). The application frequency of tensile load per hour  $n(t)$  has been maintained equal to 120. The calculated Safety Margin is close to 8, meaning this failure source is extremely unlikely, thus its effect is negligible (constant failure rate  $\lambda$  equal to 4.4E-03 failures/mln h).

A Fault Tree Analysis (FTA) can be a useful tool to resume the reliability issues described and to quantify the reliability of the piezo stack. FTA provides useful information about the likelihood of a failure (top event) occurring due to different causes [4-6, 31]. It is a procedure for determining the various combinations that can result in the occurrence of a specific undesired event at the top level. The failure of the actuator depends on different sources. For every potential cause of failure (FC), the estimated constant failure rate  $\lambda$  and the Mean Time To Repair (MTTR) are listed in Tab. 4.

TABLE 4. Likelihood of causes generating piezo failure.

Type	Source	$\lambda$ [ff/mln h]	MTTR [h]
FC1	Intrinsic failure due to fatigue	100	7
FC2	Break of the flexural joint	3.5	10
FC3	Break of the flexural springs	5 each	10
FC4	Tensile overstress	0.0044	7

For every replaceable element, exponential maintainability function  $M(t)$  is assumed, with constant repair rate  $\mu$  (the reciprocal of MTTR) [3-6, 31, 32]. Figure 8 shows the Fault Tree logic used to model the actuator reliability.

Working at the predicted conditions, the reliability of every actuator is characterized by a close-to-constant failure rate equal to 104 failures/mln h, meaning a MTTF of 9,615 h.

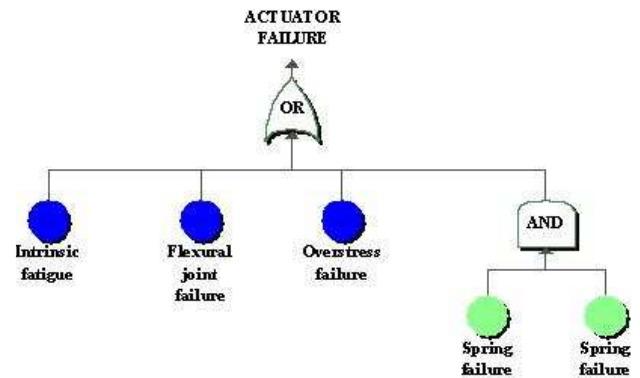


FIGURE 8. FTA of the piezo actuator.

An actuator shows a reliability of 0.515 after two years, exponentially decreasing to 0.369 after three years.  $B_{10}$  (the time by which 10% of the elements would fail [33]) is equal to 1,018 h, principally influenced by intrinsic failures. The reliability function of the actuator is shown in Fig. 9.

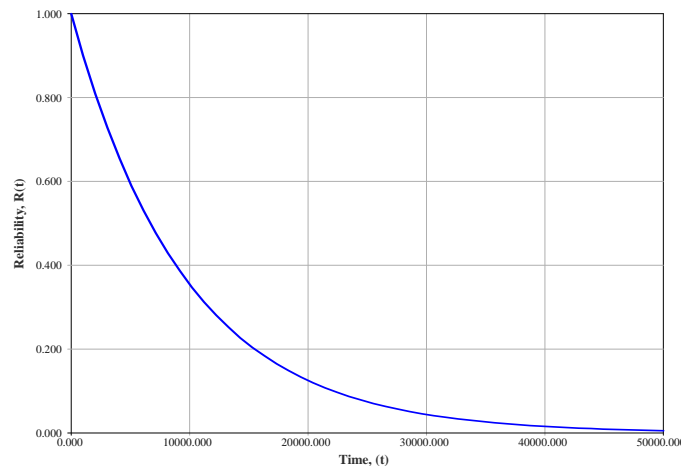


FIGURE 9. Reliability function of the actuator.

The Reliability Importance Index (IR), Eq. 7, assesses the contribution of every source of failure to the reliability  $R_s$  of the top event at a specified time. At two years, the IR for

fatigue failures is equal to 0.9769, against the 0.5268 of the flexural joint failure.

$$IR_i = \frac{\partial R_S}{\partial R_i} \quad (7)$$

### Reliability characterization of accelerometer

Since vibration monitoring and control is becoming a diffuse opportunity in industry, the accelerometers increased in precision and reliability, thanks to MEMS technological innovations. For the AVC of the SP, a triaxial smart accelerometer is needed. It must measure the displacement at the tool tip point and send signals for piezo motion, offering extremely high performances (high reliability, quick response time, humidity resistance, operating temperature 0÷80 °C and large frequency bandwidth) in a small and robust solution. The smart accelerometer is a device that includes three MEMS accelerometers, one for each of the Cartesian axis. The signals are computed by a micro processor integrated within it.

The reliability characteristics of the smart accelerometer system are achieved with Reliability Block Diagram (RBD) techniques that are unmatched for analyzing the reliability metrics of complex systems [4-6, 31, 32]. A functional block diagram lists the elements of the smart accelerometer together with their estimated failure rates (Fig. 10). These estimations are achieved from the software libraries.

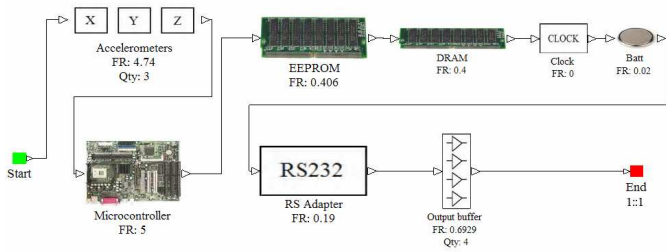


FIGURE 10. Smart accelerometer functional block diagram.

The failure of every element directly determines the failure of the system, thus the RBD is basically connected by a series configuration [4-6, 31]. The estimated MTTR is 1.5 hours.

Without considering potential failures due to the software, amplification system or connections, the smart accelerometer can be described by a high reliability (0.802 after 2 years, 0.479 after ten years), with a constant failure rate of 23 failures/mln hours. Including the entire software and hardware equipment, a mean lifetime of 40,000 hours for the entire triaxial acceleration system is reasonably assumed.

### SMART PLATFORM RELIABILITY ASSESSMENT

Since a reliable product has to guarantee performances along life cycle time, it is necessary to assess the reliability characteristics of the entire system. For the overall analysis, the SP has to be considered as a repairable system by replacing or repairing its components in a failure state [32].

In this study the SP reliability characteristics are computed basing on the morphological-functional decomposition. Once again, the reliability characteristics of SP are achieved with Reliability Block Diagram. Every failure of a component is assumed as exponentially distributed and it directly causes the

failure of the entire system. Furthermore the conditional failures for the actuators are included. Thus the RBD is connected by a series configuration, except for the smart disk system (Fig. 11). As previously mentioned, it includes two redundant gauges assembled on a steel disk (a piezo gauge and a strain one) in order to measure the piezo displacement. Every couple of gauges represents a parallel subdiagram [6, 31].

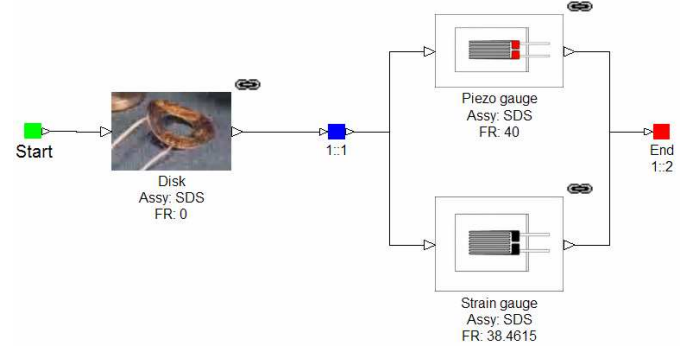


FIGURE 11. Smart Disk System subdiagram.

For RBD calculation, the failure rate of the actuators considers intrinsic and design causes (FC1 and FC4, Tab. 4) only. Table 5 shows the estimated failure rate and MTTR of the components previously unmentioned, completing the RBD architecture.

The reliability function  $R(t)$ , the instantaneous failure rate  $\lambda(t)$  and the mean availability  $A(t)$  of the SP are observed during the life cycle time (32,000 h or 10 working years).

TABLE 5. Failure rates and MTTRs for other SP components.

Element	$\lambda$ [ff/mln h]	MTTR [h]
Fixed platform	$\cong 0.0$	8.00
Mobile platform	$\cong 0.0$	5.00
Cooler joint	12.50	3.00
C-shaped plate	0.10	3.50
Steel Disk	$\cong 0.0$	7.00
Piezo gauge	40.00	7.00
Strain gauge	38.46	7.00
Temp. sensor	0.0102	6.00

A Monte Carlo simulation (1,000 simulation runs) is forced to compute system reliability indexes, when mission time is set at 32,000 hours. The software calculated an approximated system MTBF equal to 2,551 h. The steady state availability  $A(\infty)$  resulted equal to 0.9972 (Fig. 12). This value refers to the inherent availability, without considering logistic and administrative delays that often occur when a repair or replace is needed [4-6, 31, 32].

The expected number of failures is 13, equivalent to a total downtime of 88.4 h. The simulated number of failures of every actuator is 3.5, causing a total downtime of 22.4 h during the lifecycle.

The SP shows a smoothly increasing failure rate addressing nothing much wearout, as shown in Fig. 13. The lifetime probability density function can be described by a Weibull distribution; a shape parameter  $\beta$  equal to 1.014 and scale  $\eta$  equal to 2,403 have been estimated with the Least Square method ( $\rho = 0.99997$ ).

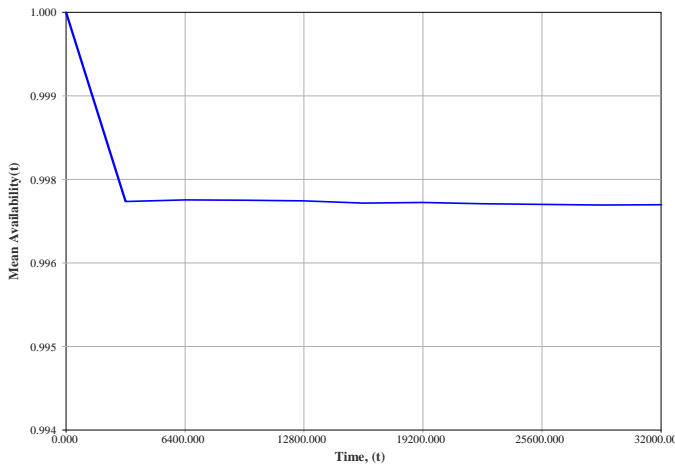


FIGURE 12. Mean availability function of the SP.

### Sensitivity Analysis and Reliability Allocation

From an industrial point of view, it is interesting to retrace down to the system tree, assessing the contributions that every group/component brings about the overall reliability characteristics. The sensitivity analysis allows to roughly understand and quantify the effect of every element on the system MTBF previously calculated. The contributions of the critical elements are estimated, “detaching” one-by-one the referred elements from the RBD and evaluating the effect on the SP reliability characteristics. An increased value means the element has a significant impact on system reliability and must be critically considered. This approach has a logical purpose, without any technical implications.

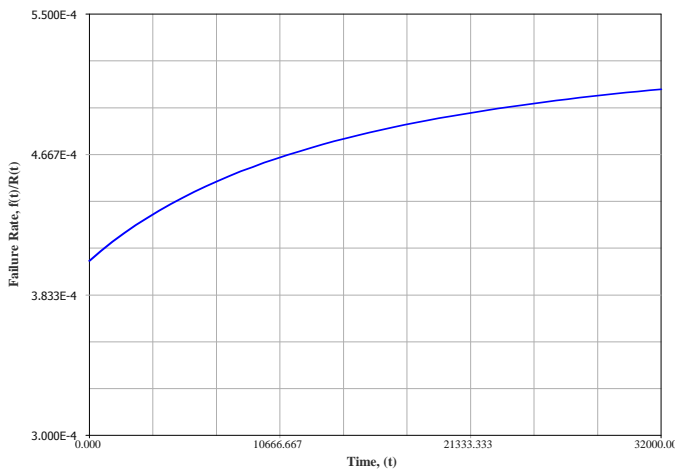


FIGURE 13. Failure Rate function of the SP.

Table 6 shows the percentage contribution on overall MTBF and the steady state availability calculated when the specified subsystem is detached. Furthermore, the Failure criticality Index (FCI) is calculated for every detached element. FCI is the ratio between the number of system downing failures of a component and the number of system failures [31]. As expected, the system MTBF is mostly affected by the failures of the piezoelectric actuators.

The achieved results imply that the reliability allocation theories [6, 31] can't drastically improve the overall performances of the SP. In fact, only machinery controls could

be added to prevent some failure sources (such as for the flexural joints and flexural springs), but the greatest impact on reliability characteristics is due to the intrinsic fatigue behavior of the piezoelectric devices.

TABLE 6. Sensitivity analysis.

Detached elements	MTBF [h]	$\Delta(\text{MTBF})$ [%]	Steady state availability	FCI [%]
3 piezo actuators	9,493	+ 272%	0.9993	25.03
3 flexural joints	2,605	+ 2.1%	0.9973	0.89
Accelerometer	2,619	+ 2.6%	0.9973	5.95
<b>None</b>	<b>2,551</b>	<b>-</b>	<b>0.9972</b>	<b>-</b>

### CONCLUSION

The paper shows how to develop a structured R&M analysis at the design stage of a complex mechanical system. The authors followed a hierarchical approach, retracing up and down the system tree and applying a series of visual and statistical tools. After dividing the system in basic elements, the most critical ones have been analyzed in detail, estimating their reliability behavior. Under the hypothesis that every element fails following an exponential distribution and when this happens it makes the system down, the reliability and maintainability of the SP has been estimated using RBD. The SP meanly fails every 9.5 working months and a high availability along the lifecycle has been calculated. The sensitivity analyses show the actuators have a great impact on the SP reliability performances, but the reliability allocation models can't be much helpful, because failures happen due to intrinsic behavior of the piezo device rather than to design lacks. The reliability modeling of the actuator is critical. The assumption the authors made have to be carefully verified following an experimental campaign and analyzing the lifedata.

Finally, since most of the probabilistic costs are directly related to the R&M characteristics, the Life Cycle Cost could be easily estimated. The variable costs of operating strictly depend on availability, the maintenance costs to the total downtime and to the number of failure per element, the spare part storage cost to the number of failure per element. Different scenarios can be achieved by introducing maintenance (preventive or corrective), replacement policies and additional information; in this manner, the improvement guidelines become driven by both technical and economical requirements.

### NOMENCLATURE

- A, n = coefficients of Black's equation
- A(T) = mean availability
- A( $\infty$ ) = steady state availability
- B<sub>x</sub> = time equivalent to x% unreliability
- E = applied electric field
- k = Boltzmann's constant
- L(s) = distribution of stresses
- M(t) = maintainability function
- MTBF = mean time between failures
- MTTF = mean time to failure
- MTTR = mean time to repair
- n(t) = loads per time units
- R(t) = reliability function
- s = load
- SM = safety margin



$S(s)$  = distribution of strengths  
 $t$  = time (or cycles)  
 $T$  = absolute temperature  
 $W$  = activation energy  
 $\beta$  = shape parameter of the Weibull distribution  
 $\eta$  = scale parameter of the Weibull distribution  
 $\lambda$  = parameter of exponential distribution  
 $\lambda(t)$  = failure rate function  
 $\mu(t)$  = repair rate function  
 $\mu_L, \sigma_L$  = mean and standard deviation of stress  
 $\mu_P, \sigma_P$  = mean and standard deviation of preload  
 $\mu_S, \sigma_S$  = mean and standard deviation of strength  
 $\mu_T, \sigma_T$  = mean and standard deviation of tensile stress  
 $\rho$  = correlation coefficient for Least Square regression

## REFERENCES

- [1] Bernstein, N., 1985, "Reliability Analysis Techniques for Mechanical Systems", Quality Reliability Engineering International, Vol.1(4), pp.235-248.
- [2] Stamatis, D.H., 1995, *Failure mode and effect analysis*, ASQ Quality Press, Milwaukee, WI.
- [3] Smith, D. J., 2001, Reliability, Maintainability and Risk, Butterworth Heinemann, Oxford, UK.
- [4] Ebeling, C., 1997, An introduction to reliability and maintainability engineering, Waveland, Long Grove, IL.
- [5] O'Connor, P. D. T., 1991, Practical Reliability Engineering, John Wiley & sons, New York, NY.
- [6] Pecht, M., 1995, Product Reliability, Maintainability, and Supportability Handbook, CRC, New York, NY.
- [7] Colla, E.L., Suyal, G., Gentil, S., and Setter, N., 2004, "Highly Efficient Piezoelectric Actuators for Active Vibration Control", Proceedings of Materials Research Society, Vol. 785, pp. 11-22.
- [8] Luo, Y., Xie, S., and Zhang, X., 2008, "The actuated performance of multi-layer piezoelectric actuator in active vibration control of honeycomb sandwich panel", Journal of Sound and Vibration, Vol.317, pp. 496-513.
- [9] Moshrefi-Torbati, M., Keane, A.J., Elliott, S.J., Brennan, M.J., Anthony, D.K., and Rogers E., 2006, "Active vibration control (AVC) of a satellite boom structure using optimally positioned stacked piezoelectric actuators", Journal of Sound and Vibration, Vol.292, pp.203-220.
- [10] Palazzolo, A.B., Lin, R.R., Alexander, R.M., Kascak, A.F., and Montague, J., 1991, "Test and theory for piezoelectric actuator-active vibration control of rotating machinery", Journal of Vibration and Acoustics, Vol.113, pp.167-175.
- [11] Merlo, A., Mazzola, M., Aggogeri, F., Brunner, B., and De la O Rodriguez, M., 2008, "A structured analysis for the reliability prediction of a micromilling machine subsystem", Proceedings of 8th Advanced Manufacturing Systems and Technology conference, Udine, Italy.
- [12] Ford Motor Company, 1996, Failure Mode & Effects Analysis. Handbook supplement for machinery, FMC release, Dearborn, MI.
- [13] Ashby, M.F., 2005, Materials selection in mechanical design, Butterworth-Heinemann, Oxford, UK.
- [14] Carter, A.D.S., 1986, Mechanical reliability, Macmillan, London, UK.
- [15] Swift, K.G., Raines, M., and Booker, J.D., 2001, "Advances in Probabilistic Design: manufacturing knowledge and applications", Journal of Engineering Manufacture - Part B, Vol. 215, pp.297-313.
- [16] Pritchard, J., Bowen, C.R., and Lowrie, F., 2001, "Multilayer actuators: review", British Ceramic Transactions, Vol.100 (6), pp.1-9.
- [17] Uchino, K., 1997, Piezoelectric Actuators and Ultrasonic Motors, Kluwer, Boston, MA.
- [18] Uchino, K., 2000, Ferroelectric devices, CRC PRESS, Boca Raton, FL.
- [19] Van den Ende, D.A., Bos, B., Groen, W.A., and Dortmans, L.M.J.G., 2007, "Lifetime of piezoceramic multilayer actuators: Interplay of material properties and actuator design", Proceeding of International Conference on Electroceramics, Arusha, Tanzania.
- [20] Fouiday, M., Saki, M., Hammoudi, N., Simonet, L., and Saugnac, H., 2006, "Electromechanical Characterization of Piezoelectric Actuators Subjected to a Variable Preloading Force at Cryogenic Temperature", Proceedings of EPAC 2006, Edinburgh, Scotland.
- [21] Chaplya, P.M., Mitrovic, M., Carman, G.P., and Straub, F.K., 2006, "Durability Properties of Piezoelectric Stack Actuators under Combined Electro-Mechanical Preload", Journal of Applied Physics, Vol.100, 124111.
- [22] Nagata, K., and Kinoshita, S., 1995, "Relationship between Lifetime of Multilayer Ceramic Actuator and Temperature", Japanese Journal of Applied Physics, Vol.34, pp.5266-5269.
- [23] Polcawich, R., and Trolier-McKinstry, S., 2000, "Piezoelectric and dielectric reliability of lead zirconate titanate thin films", Journal of Material Research, Vol.15 (11), pp.2505-2513.
- [24] Sakai, T., Kawamoto, H., 1998, "Durability properties of Piezoelectric Stack Actuator", Japanese Journal of Applied Physics, Vol.37, pp.5338-5341.
- [25] Thorengrueng, J., Tsuchiya, T., and Nagata, K., 1998, "Lifetime and Degradation Mechanism of Multilayer Ceramic Actuator", Japanese Journal of Applied Physics, Vol.37, pp.5306-5310.
- [26] Uchino, K., 1998, "Materials Issues in design and performance of piezoelectric actuators: an overview". Acta Mater, Vol.46 (11), pp.3745-3753.
- [27] Koh, J.H., Jeong, S.J., Ha, M.S., and Song, J.S., 2004, "Lifetime and reliability of Pb(Mg,Nb)O<sub>3</sub>-Pb(Zr,Ti)O<sub>3</sub> multilayer ceramic piezoelectric actuators", Japanese Journal of Applied Physics, Vol.43, pp.6212-6216.
- [28] Koh, J.H., and Kim, T., 2006, "Reliability of Pb(Mg,Nb)O<sub>3</sub>-Pb(Zr,Ti)O<sub>3</sub> multilayer ceramic piezoelectric actuators by Weibull method", Microelectronics Reliability, Vol.46, pp.183-188.

- [29] Pertsch, P., Richter, S., Kopsch, D., Krämer, N., Pogodzic, J., and Henning, E., 2006, "Reliability of Piezoelectric Multilayer Actuator", Proceedings of Actuator 2006 Conference, Bremen, GER.
- [30] Andersen, B., Jensen, F., and Ouchouche, S., 2004, "Reliability of Piezoelectric Actuators at Extreme Operating Conditions", Proceedings of Actuator 2004 Conference, Bremen, Germany.
- [31] ReliaSoft Corporation, 2005, System Analysis Reference: Reliability, Availability & Optimization, Reliasoft Publishing, Tucson, AZ.
- [32] Rigdon, S.E., and Basu, A.P., 2000, Statistical Methods for the Reliability of Repairable Systems, Wiley Interscience, New York, NY.
- [33] Harris, T.A., 1991, Rolling Bearing Analysis, John Willey & Sons, New York, NY.